Biol. Cybern. 78, 95–106 (1998)

Biological Cybernetics

A cross-interval spike train analysis: the correlation between spike generation and temporal integration of doublets

David C. Tam

Center for Network Neuroscience and Department of Biological Sciences, University of North Texas, P.O. Box 305220, Denton, TX 76203-5220, USA

Received: 3 March 1997 / Accepted in revised form: 6 November 1997

Abstract. A stochastic spike train analysis technique is introduced to reveal the correlation between the firing of the next spike and the temporal integration period of two consecutive spikes (i.e., a doublet). Statistics of spike firing times between neurons are established to obtain the conditional probability of spike firing in relation to the integration period. The existence of a temporal integration period is deduced from the time interval between two consecutive spikes fired in a reference neuron as a precondition to the generation of the next spike in a compared neuron. This analysis can show whether the coupled spike firing in the compared neuron is correlated with the last or the second-to-last spike in the reference neuron. Analysis of simulated and experimentally recorded biological spike trains shows that the effects of excitatory and inhibitory temporal integration are extracted by this method without relying on any subthreshold potential recordings. The analysis also shows that, with temporal integration, a neuron driven by random firing patterns can produce fairly regular firing patterns under appropriate conditions. This regularity in firing can be enhanced by temporal integration of spikes in a chain of polysynaptically connected neurons. The bandpass filtering of spike firings by temporal integration is discussed. The results also reveal that signal transmission delays may be attributed not just to conduction and synaptic delays, but also to the delay time needed for temporal integration.

1 Introduction

Recently, multineuron recordings have been developed, such as multiunit extracellular recording in vivo (Gerstein et al. 1982; Novak and Wheeler 1986; Nicolelis et al. 1993, 1995, 1997; Nicolelis and Chapin 1994), multiunit extracellular recording in vitro (Droge et al. 1986; Gross 1994; Tam and Gross 1994a), and multichannel optical recording (Cohen and Lesher 1986; Nakahama et al. 1992), which are useful in understanding the structure and function of a neuronal network. The relationship of the spike firing activities between two neurons detected by the multineuron recordings was traditionally analyzed by cross-correlation techniques. One of the most commonly used correlation analyses in neurophysiology is the conventional cross-correlation analysis (Perkel et al. 1967a, b) and its derivative measures, such as the scaled cross-coincidence histogram (Melssen and Epping 1987), the cross-covariance histogram (Palm et al. 1988), the joint peristimulus time histogram (Aertsen et al. 1989), the cross-interspike interval histograms (Tam et al. 1988), the preconditional cross-interval histogram (Gross and Tam 1994), and the postconditional cross-interval histogram (Tam and Gross 1994b). However, there are some difficulties with these cross-correlational methods (Yang and Shamma 1990). They are focused on extracting the relationship of one-to-one coupled spike firings in neurons. That is, the coupling between two neurons is established by correlating a *single-spike* firing of one neuron to the probability of the next single-spike firing in another neuron. The contribution of *multiple-spike* firing to single-spike coupled firing has yet to be addressed. In particular, the phenomenon of temporal summation in synaptic integration is an example of a multiple-spike to single-spike coupled-firing relationship. Although temporal integration is a well-known phenomenon, its implications have not been fully studied until recently (e.g., experimentally by Softky and Koch 1993, and theoretically by Kudela et al. 1997). Yet, most spike-train analyses were not designed specifically to extract the temporal summation of spike firing in a neuron. Conventional cross-correlation techniques (or other similarly derived correlation statistics) primarily correlate the single-spike to single-spike firing relationship between neurons. Since temporal summation implies the integration of multiple spikes over time, such a contribution to the spike firing can only be obtained if the correlation spike-train analysis method also includes the probability of firing based on not just one preceding spike, but multiple spikes.

A spike-train analysis technique is introduced here to address the relationship between the probability of a spike generated in one neuron and the possible contribution of integrating two consecutive spikes fired from another neuron. In other words, the likelihood of spike generation that

Correspondence to: D.C. Tam (e-mail: dtam@unt.edu, Tel.: +1-940-565-3261, Fax: +1-940-565–4136)

can be attributed to temporally integrating multiple spikes is sought by correlating the next spike firing time of a 'compared' neuron with the time interval between the previous consecutive firings in a 'reference' neuron.

We will derive the statistics of spike firing times in this pair of neurons so that the conditional probability of spike firing can be established in relation to the integration period. The existence of a temporal 'integration period' is revealed by the probability that the compared neurons will generate a spike that is conditional to the prior firing of two consecutive spikes in the reference neuron. A preconditional correlation statistic is established to estimate the conditional probability of spike firing in the compared neuron given that the reference neuron has fired not just a *single* spike, but *two* sequential spikes. Thus, the focus of this analysis is to address the likely contribution of *two* successive spikes (i.e., a doublet) that may be summated to generate the next spike. By correlating this doublet firing interval, the integration period associated with either the excitation or the suppression of spike firing in a neuron can be revealed with this analysis.

Alternatively, this analysis can be considered as correlating the relationship between the time intervals of spike firings. The time interval between spike firings of the same neuron is called the interspike interval (ISI) and the time interval between spike firings of a reference and a compared neuron is called the cross-interval (CI) (see Fig. 1). The conditional and joint probability of spike firing can be estimated from these ISI and CI statistics to deduce the integration period from the reference neuron's ISI prior to the compared neuron's next spike firing. This happens if the ISI is correlated with the coupling latency, which is revealed by this correlated CI.

2 Methods

2.1 Overview

We call this temporal integration of doublet spike train analysis the 'pre-ISI/post-CI analysis,' because it establishes the relationship between the pre-ISI and post-CI by the conditional (and joint) probability of spike firing between two neurons. By examining the firing probability of the compared neuron's next spike relative to the reference neuron's ISI duration (whose relationship is shown by the thick arrows in Fig. 1), the conditional probability can be established in relation to the time interval in which two preceding spikes may have been integrated (or summated) to produce this next spike firing if these neurons are synaptically connected. As in cross-correlation analysis, the firing probability of a spike in a compared neuron is estimated by the statistics obtained from the firing times of the compared and reference neurons.

2.2 Definitions

Given two spike trains obtained from two neurons, let one of the spike trains be called the reference spike train, A, and the other the compared spike train, B. Let us assume that there is a total of N_A spikes in train A, and N_B spikes in train B, then the spike trains can be represented by

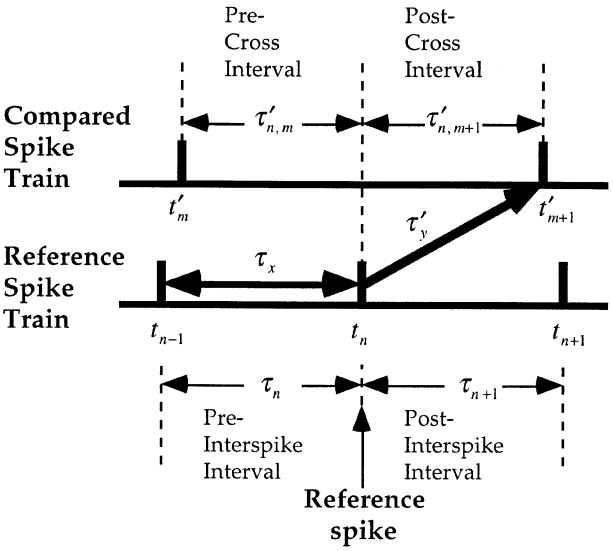

Fig. 1. Schematic diagram of two spike trains showing the relationships between the interspike intervals (ISI) and cross-intervals (CI) relative to a reference spike. The timing relationship between the reference and compared neurons' firing (indicated by the *thick single arrow* representing the post-CI) can be correlated with the temporal integration period of a doublet (indicated by the *thick double arrow* representing the pre-ISI) by the pre-ISI/post-CI analysis

$$x_A(t) = \sum_{n=1}^{N_A} \delta(t - t_n) \tag{1}$$

and

$$x_B(t) = \sum_{m=1}^{N_B} \delta\left(t - t'_m\right) \tag{2}$$

$\forall t_n, t'_m$ such that $t_n < t_{n+1}$ and $t'_m < t'_{m+1}$

where t_n and t'_m are the times of occurrence of n-th and m-th spikes in spike trains A and B, respectively, and $\delta(t)$ is a Dirac delta function denoting the occurrence of a spike at time t. Note that we use the primed notation to denote the times of spike occurrence in spike train B and CIs between the two spike trains.

The relationships between the ISIs and the CIs with respect to the reference neuron is shown in Fig. 1. Note that there are two ISIs defined with respect to a reference spike: one before and one after. The pre-ISI relative to the n-th reference spike in train A is defined as

$$\tau_n = |t_{n-1} - t_n| \tag{3}$$

Similarly, there are two CIs defined with respect to a reference spike. The post-CI between the compared and reference spike trains relative to the n-th reference spike in spike train A is defined as

$$\tau'_{n,m+1} = |t'_{m+1} - t_n| \tag{4}$$

for $t'_m < t_n \leq t'_{m+1}$.

The probability that the next spike will fire at time τ after a reference spike has fired is described by the probability density function (pdf) of the next spike firing. The probability that a compared neuron will fire the next spike

at time τ'_y after the reference neuron has fired two spikes (one reference spike at time zero, and another at time τ_x prior to the reference spike) is described by the joint pdf. This joint pdf is estimated from the following:

$$P\left(\tau_x \cap \tau'_y\right) = \frac{\sum_{n=2}^{N_A} \delta\left(|t_{n-1} - t_n| - \tau_x\right) \delta\left(|t'_{m+1} - t_n| - \tau'_y\right)}{N_A - 1} = \frac{\sum_{n=2}^{N_A} \delta\left(\tau_n - \tau_x\right) \delta\left(\tau'_{n,m+1} - \tau'_y\right)}{N_A - 1} \quad (5)$$

$\forall t_n, t'_m$ such that $t'_m < t_n \leq t'_{m+1}$ and $t_{n-1} < t_n$ where τ_x is the 'lead time' and τ'_y the 'lag time' as defined in conventional correlation terminology (Perkel et al. 1967a, b). The correlation between the post-CI and the pre-ISI is captured by this joint pdf. In other words, the likelihood of the compared neuron firing the next spike is correlated with the previous two spikes fired by the reference neuron. Similarly, the conditional pdf is estimated from the following:

$$P\left(\tau_x|\tau'_y\right) = \frac{\sum_{n=2}^{N_A} \delta\left(|t_{n-1} - t_n| - \tau_x\right) \delta\left(|t'_{m+1} - t_n| - \tau'_y\right)}{\sum_{n=2}^{N_A} \delta\left(|t'_{m+1} - t_n| - \tau'_y\right)} = \frac{\sum_{n=2}^{N_A} \delta\left(\tau_n - \tau_x\right) \delta\left(\tau'_{n,m+1} - \tau'_y\right)}{\sum_{n=2}^{N_A} \delta\left(\tau'_{n,m+1} - \tau'_y\right)} \quad (6)$$

Both the joint pdf and the conditional pdf can be represented graphically by a two-dimensional function displayed in an xy-plot. Alternatively, a scatter plot with dots representing the coordinate $\left(\tau_x, \tau'_y\right)$ of individual points in the numerator of (5) or (6) can be used to represent the non-normalized joint distribution similar to the scatter plot traditionally used in the joint interspike interval (JISI) analysis (Rodieck et al. 1962). Other similar methods include the 'return map' in nonlinear dynamics analysis (Selz and Mandell 1992; Smith 1992), the preconditional cross-interspike interval analysis (Tam et al. 1988), and the postconditional cross-interval analysis (Tam and Gross 1994b). In other words, a pre-ISI vs post-CI scatter plot is produced by taking each spike in the reference spike train as the reference spike and plotting each corresponding point with the $\left(\tau_x, \tau'_y\right)$ coordinate representing the pre-ISI and the post-CI pair on the xy-plot. The $\left(\tau_x, \tau'_y\right)$ coordinate of a point in this xy-plot is given by $\left(|t_{n-1} - t_n|, |t'_{m+1} - t_n|\right)$ for the n-th reference spike.

2.3 Interpretations

When points are plotted on the pre-ISI vs the post-CI graph, clusters and/or bands of points may appear when the same firing pattern is repeated. Conversely, points missing in a certain region of the plot indicate patterns of suppressed spike firing. Depending on a point's location and orientation in the graph, specific spike firing patterns between neurons can be inferred. Clustering of points at coordinate $\left(\tau_x, \tau'_y\right)$ indicate that the compared neuron is coupled with the previous firing of two spikes in the reference neuron. This tight coupling occurs only when the reference neuron fires a doublet at exactly τ_x ms apart.

Figure 2A shows how the different orientation of bands of points can be interpreted with respect to the spike firing patterns. Points aligned horizontally indicate that the post-CIs are constant, i.e., there is a constant latency between the firing of spikes in the two neurons given by

$$\tau'_y = c \quad (7)$$

where c, the lag time, is a constant (Fig. 2B). If points are confined within a limited range of pre-ISIs $< \tau_2$ (such as the points *a*, *b*, *c*, and *d* in Fig. 2B), then this indicates that the compared neuron's firing is coupled with the reference neuron's firing only when the reference neuron has fired two spikes within this ISI of τ_2. This means that the integration period associated with the next spike firing in the compared neuron is τ_2, because the compared neuron's next spike firing happens at lag time c only when the reference neuron fired two previous spikes within this period, not outside this period. Note that the horizontal band of points is usually delimited by τ_1 and τ_2 due to the fact that a second spike cannot be fired within the refractory period, τ_1, even though the total integration time is still τ_2.

Points lying along a vertical line indicate that the ISIs are constant, independent of the post-CIs (Fig. 2C). This means that the reference neuron is firing periodically, uncorrelated with the compared neuron's next firing, with the period

$$\tau_x = c \quad (8)$$

where c is a constant. This means that the firing of the compared neuron is uncoupled with, and independent of, the reference neuron's preceding doublet firing.

Points lying along an antidiagonal ($-45°$) line can be represented by the following relationship:

$$\tau_x + \tau'_y = c \quad (9)$$

where c is a constant (Fig. 2D). This antidiagonal band of points shows that the firing in the compared neuron is correlated with the reference neuron's second-to-last spike firing rather than the last firing. If points are confined within the lower triangle (shaded region in Fig. 2D, where $\tau_x + \tau'_y < c$), then the firing of the next spike in the compared neurons is correlated with the firing of a minimum of two spikes within this integration period of c.

2.4 The network of simulated neurons

A network of simulated neurons whose spike trains are generated by stochastic point processes is used in our analysis below. In brief, neuron A is the driver neuron connected directly to neurons B, C, E, and F, and indirectly to neuron D via B. The connections are all excitatory except for neuron F, which is inhibitory. The spike trains of driver neuron A and driven neuron F are generated by a Poisson process, simulating spontaneous random firing, while the other neurons, B, C, D, and E, are driven without any spontaneous firing.

A larger recurrent network could be used to illustrate the capacity of this new analysis, but it would create complications of 'cause-and-effect' interpretations in a mutually

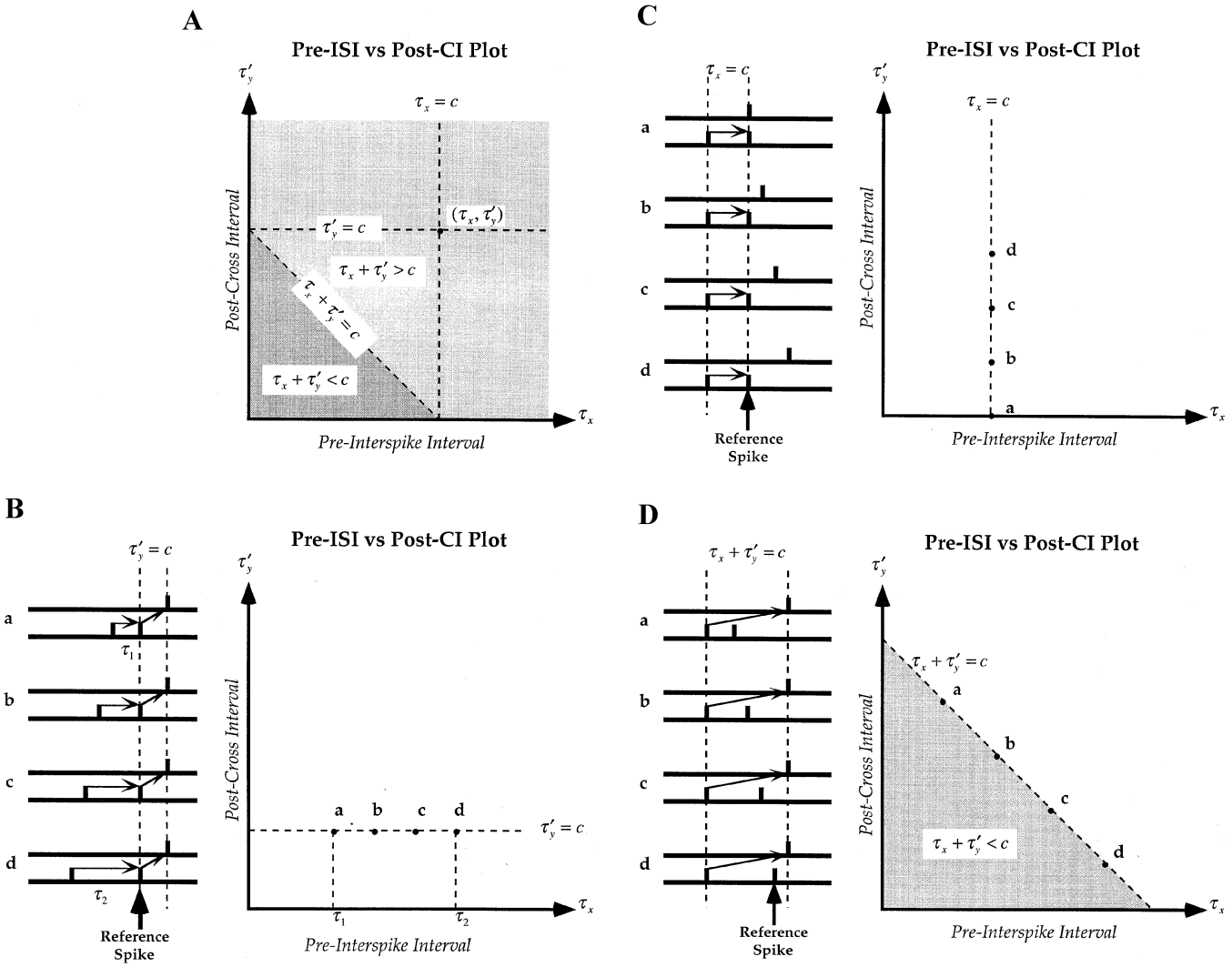

Fig. 2. Pre-ISI vs post-CI plot showing **A** various relationships between the pre-ISIs and post-CIs, **B** points lying along a horizontal line, **C** points lying along a vertical line, and **D** points lying along an antidiagonal ($-45°$) line that correspond to the spike firing patterns shown on the *left*

reciprocally connected network because neurons are driven by one another as well as being drivers themselves in such situations. Furthermore, correlation is a necessary, but not sufficient, condition to prove causality or anatomical connectivity. Therefore, we will limit our simulations to deducing *functional* connectivity using correlation analysis so that the signal processing capability of a neural network can be revealed based on the interactions of neurons within a network.

3 Results

3.1 Uncovering the temporal integration period

Figure 3A shows the pre-ISI/post-CI scatter plot for neuron A (used as the reference neuron) compared with neuron B, which has a coupling probability of 100%, an integration time of 10 ms, and a conduction delay of 2.5 ms. A horizontal band of points at 2.5 ms post-CI latency is found within 4 and 10 ms pre-ISIs; this is congruent with the fact that the firing of neuron B is completely coupled to neuron A when the integration period is within 10 ms. Within this period (pre-ISI < 10 ms), all points fall within the horizontal band of 2.5 ms post-CIs. When the integration period is over (pre-ISI > 10 ms), points are scattered at other post-CIs, which indicates that the spike firing in neuron B is no longer time-locked to the previous firing of the driver neuron A.

The characteristic distribution of points in the pre-ISI/post-CI scatter plot of Fig. 3A can be explained by the various spike firing relationships for the two neurons depicted in Fig. 3B that correspond to the regions in the pre-ISI/post-CI scatter plot. Region a represents the refractory period of neuron A where no points are found. Region b represents the time-locked coupling between the firing in neuron B and the preceding firings in neuron A. This occurs only when neuron A fires two preceding spikes within the 10 ms corresponding to the integration time window. No points are found in region d because when the ISI between the two preceding spikes exceeds the integration period (pre-ISI > 10 ms), neuron B will not be driven to fire a spike by neuron A. Note that the integration period is not revealed by the post-CI histogram (or analogously cross-correlogram, which sums

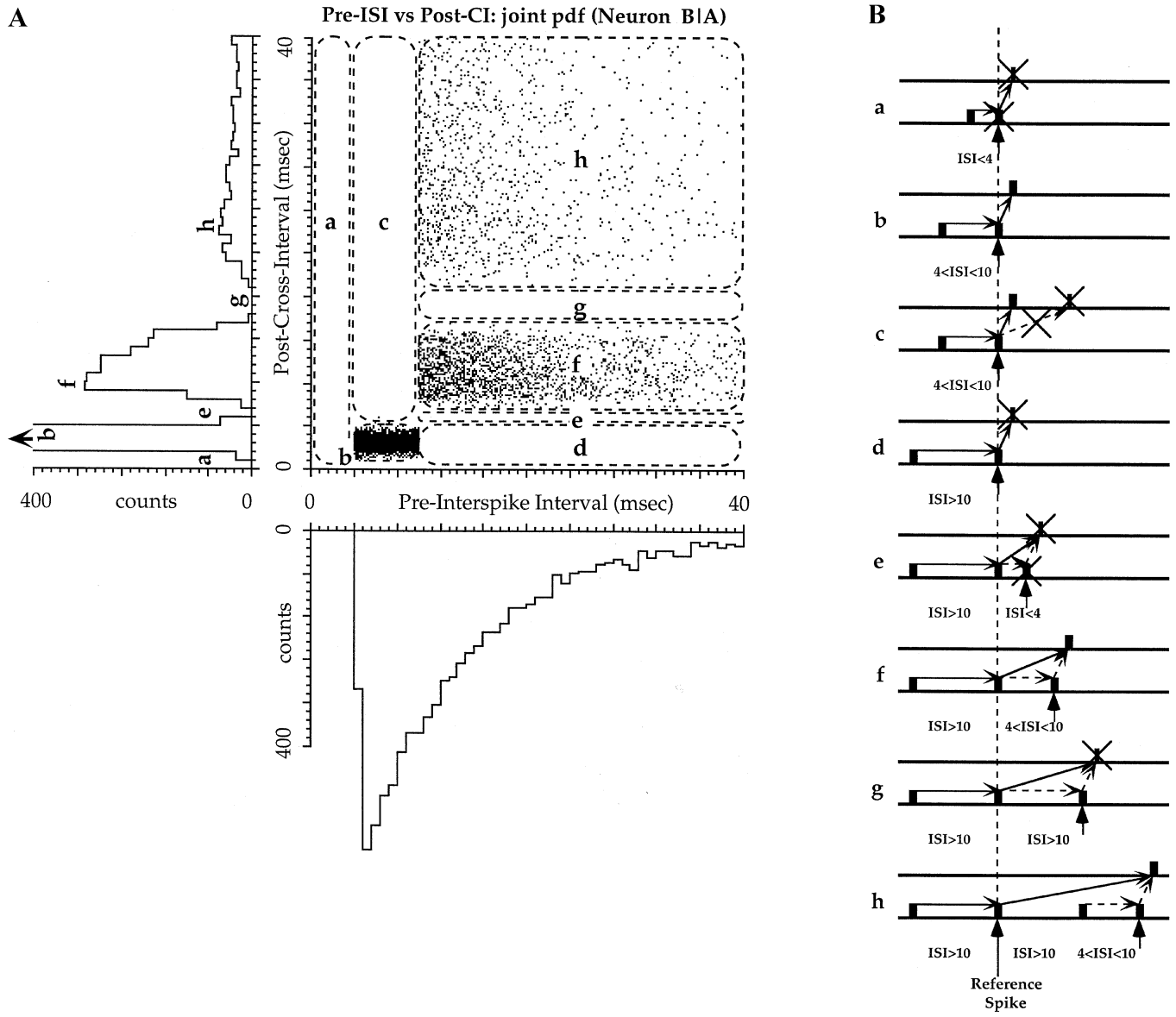

Fig. 3. A Pre-ISI vs post-CI scatter plot for neuron A as the reference neuron and neuron B as the compared neuron with 100% coupling probability strength. Note the horizontal band of points at 2.5 ms post-CI between 4 and 10 ms pre-ISI that reveals the integration period of doublet firing in the presynaptic neuron A. Note also the other horizontal band of points for pre-ISI $>$ 10 ms and the corresponding multimodal distribution in the post-CI histogram. **B** Schematic diagrams showing the temporal relationship of firing patterns corresponding to the regions depicted in the pre-ISI/post-CI scatter plot and the post-CI histogram. The *lower spike trains* represent neuron A's firing while the *upper spike trains* represent neuron B's firing. The *arrow* at the peak of the post-CI histogram indicates that the peak is extended beyond the displayable region of the graph

all n-th order CI histograms), but revealed distinctly by the pre-ISI/post-CI scatter plot.

3.2 Effects of tightly coupled firing

Points would be found in the incomplete coupled region c if the firing of the driven neuron is not tightly coupled to the driver (with a coupled firing probability $<$ 100%). In this example, no points are found in this region because neuron B's firing is completely coupled with neuron A's, whereas for neuron D, to be discussed below (see Fig. 6), points are found in region c due to the dropout of the one-to-one spike-following relationship.

When neuron B fails to follow neuron A's firing, the post-CI would be longer than 2.5 ms. This only happens when the pre-ISI is longer than the 10 ms integration period (regions f and h). This failure in coupling is expected due to the fact that neuron B cannot follow neuron A's firing when there is only *one* spike to integrate within the integration period. This shows that the pre-ISI/post-CI analysis can reveal whether the coupled firing probability is 100% or not, and when failure in spike-following occurs, the analysis further reveals whether or not that failure is due to insufficient spikes for temporal summation.

3.3 Effects of temporal integration time-delay

The coupled firings between the neuron pair can alternatively be characterized by the post-CI histogram (left histogram of

Fig. 3A). Note that the post-CI histogram shows an multimodal distribution rather than a unimodal distribution (peaking at 2.5 ms latency) if neuron B does not integrate temporally. The sharp peak at 2.5 ms post-CI is expected since this reflects the latency of the 2.5-ms time-locked firing between the two neurons. The other distributions at longer latencies (regions f and h) are not correlated with the 10-ms temporal integration period. These coupled firings at longer latencies than 2.5 ms are the result of the correlation with the driver's second-to-last spike (or other previous spikes) as shown by the firing relationships f and h depicted in Fig. 3B. These long latency delays can be attributed to the additional time that the driven neuron takes to integrate multiple spikes before it fires as depicted by the relationship f in Fig. 3B.

3.4 Effects of temporal integration of random firing on the driven neuron

The firing characteristics of the driven neuron, as revealed by the ISI histogram, is distinctly different from that of the driver neuron even though the neurons are tightly coupled. This can be inferred from the ISI distribution of the driven neuron, B, which is multimodal (Fig. 4A) and quite different from the Poisson ISI distribution of the driver neuron, A (bottom histogram of Fig. 3A). This difference in firing characteristics is a seemingly unexpected consequence of temporal integration of the driven neuron because the analysis revealed that a randomly firing driver neuron can produce rather regularly firing intervals in the driven neuron even when they are tightly coupled. The regularity of the firing of neuron B is revealed by the prominent peak (between 4 and 10 ms) in the ISI histogram (Fig. 4A).

The significance of this finding is that regularity in spike firing can be driven by irregularly firing neurons in a network by taking advantage of the temporal integrative property of the 'downstream' (driven) neuron. The periodicity of the driven neuron is a function of the temporal integration period of the driven neuron and the refractory period of the driver neuron. The preferred firing ISIs of the driven neuron is delimited by the refractory period of the driver neuron (4 ms in this example) and the integration period of the driven neuron (10 ms in this example). Therefore, this example illustrates that random spike firing in a network does not necessarily produce random firing in the driven neuron, but fairly regular firing patterns. Furthermore, this example demonstrates that the firing characteristics of the driven neuron can be quite dissimilar from the driver neuron, even for a neuron whose spike firing activity is completely dependent on a single driver neuron.

3.5 Effects of the coupling relationship with the last or second-to-last spike firing

Figure 5 shows the pre-ISI/post-CI scatter plot for neuron A used as reference neuron in relation to neuron C. The firing characteristic of neuron C is similar to that of neuron B, except that the conduction delay between neurons A and C is 15 ms rather than 2.5 ms as in neuron B. The pre-ISI/post-CI scatter plot in Fig. 5 shows additional features of

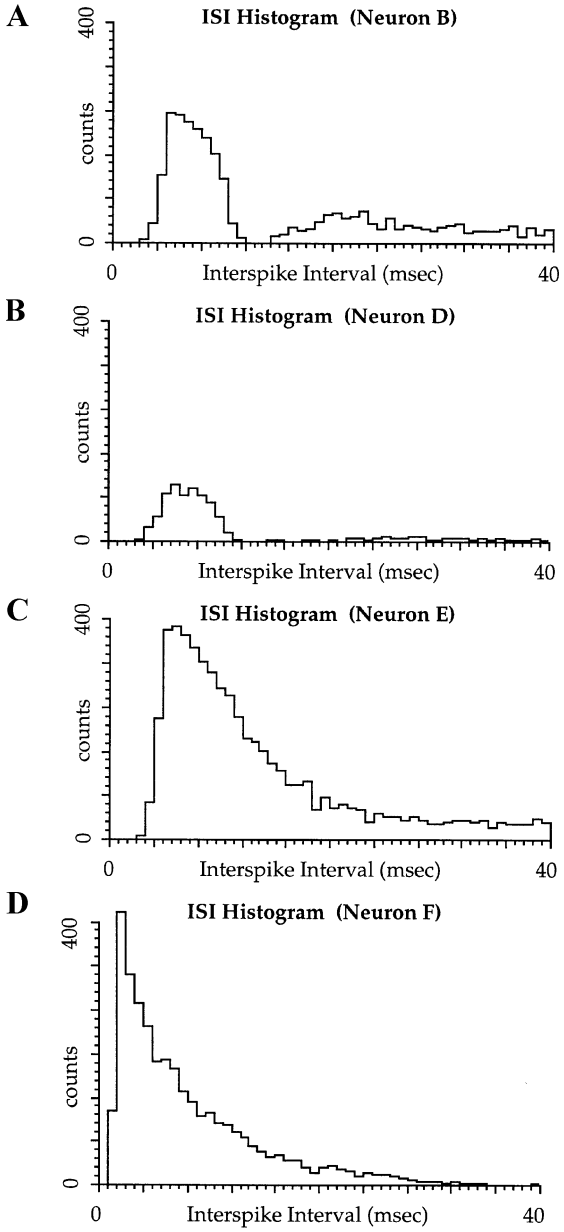

Fig. 4. Interspike interval histograms of the driven neurons showing: fairly regular firing for the monosynaptically driven neuron B **A**, very regular firing for the polysynaptically driven neuron D **B**, irregular firing for neurons E with gradual integration period **C**, and irregular firing for the inhibited neuron F **D**

an antidiagonal ($-45°$) band of points and a lower triangular distribution of points when compared with Fig. 3A.

The antidiagonal band of points indicates that the spike firing in neuron C is time-locked to the *second-to-last* spike firing in neuron A rather than the *last* (see also interpretations in Sect. 2.3 and Fig. 2D). This is due to the fact that since the latency is rather long (15 ms), there are often intervening spikes being fired in neuron A during this latency period. As a result of the intervening spikes firing during the latency period, the correlation between the time of occurrence of the next cross-spike with the preceding firing in the reference neuron may be interrupted by these intervening spikes. This results in the artifact of correlating spike firings with the second (or earlier) preceding spike instead

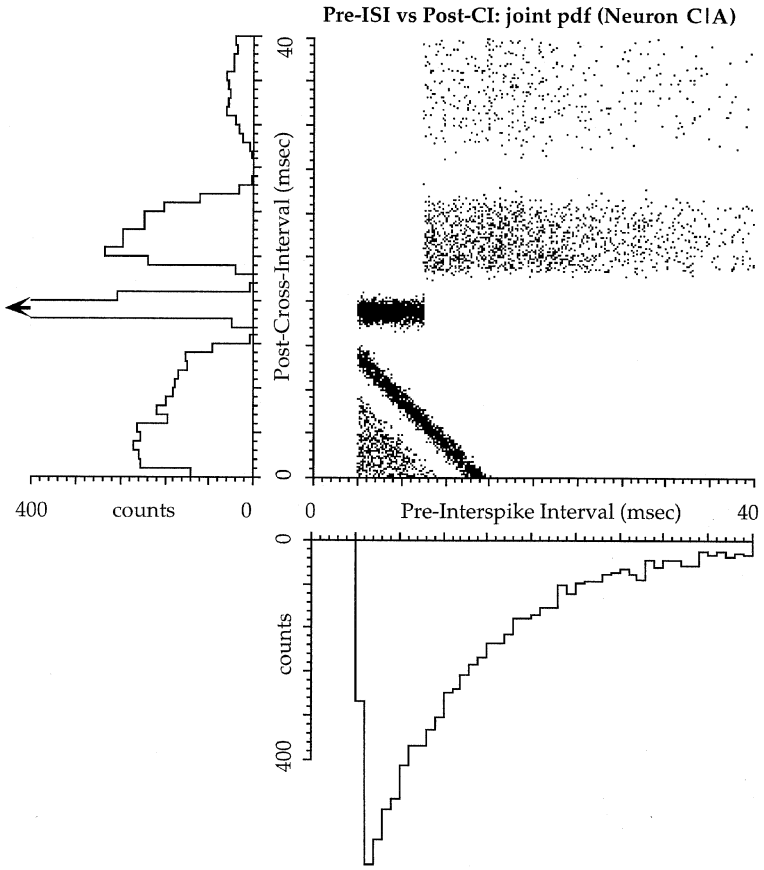

Fig. 5. Pre-ISI vs post-CI scatter plot for neuron A as the reference neuron and neuron C as the compared neuron with 100% coupling probability strength similar to neuron B except for the longer latency. Also, note the similarity between this figure and Fig. 4, except for the anti-diagonal band of points at the lower left triangle due to the longer latency of spike-following, which results in a correlation between the second-to-last preceding spike instead of the immediately preceding spike in neuron A

of the first preceding spike. This resulting artifact is actually another advantage of using this pre-ISI/post-CI analysis to detect the correlation of spike firing with the *second* preceding spike, which other correlation analyses, such as CI histogram or cross-correlogram, may not reveal so distinctly.

The post-CI histogram (left histogram of Fig. 5) reveals a multimodal distribution. The sharp peak at the 15 ms latency reveals the tightly coupled spike-following of neuron C, but does not distinguish whether such time-locked coupling is correlated with the first or second preceding spike firing, nor does it reveal the fact that the coupling is correlated with the temporal summation of two preceding spikes as extracted by the pre-ISI/post-CI scatter plot. Upon examining the corresponding antidiagonal band of points in the pre-ISI/post-CI scatter plot, the conclusion can be made that the coupling is related to the previous reference spike instead of the current reference spike (see also interpretations in Sect. 2.3). These results illustrate the advantage of using the pre-ISI/post-CI analysis, which distinguishes whether the time-locked spike firing in the compared neuron is (1) correlated with a *single* preceding spike, (2) correlated with *two* preceding spikes in the reference neuron, or (3) correlated with an *integration time window* delimited by the two previous reference spike firing times.

3.6 Effects of polysynaptic coupling with temporal integration

To show the effects of polysynaptic coupling on a network, we analyzed the firing pattern of neuron D, which is driven by neuron A indirectly via neuron B. Neurons B and D are identical with respect to their temporal integration period and conduction latency. The 10 ms integration period can be revealed by the distinct horizontal band in the pre-ISI/post-CI plot (Fig. 6), similar to the previous neurons (cf. Figs. 3A and 5). The difference between monosynaptically and polysynaptically coupled temporal integrations can clearly be revealed by this new analysis (by comparing Figs. 3A and 6). Whereas temporal integration for neuron B is coupled to the 2.5 ms conduction latency with the driver neuron A (revealed by a band of points at 2.5 ms post-CI), temporal integration for neuron D is coupled to a much wider range of latencies between 5 ms (= 2.5 + 2.5) and 15 ms (= 2.5 + 2.5 + 10). That is, the latency is not just the sum of the two 2.5 ms polysynaptic conduction latencies, but also the addition of the 10 ms integration period of neuron B. This additional delay is due to the integration time taken for neuron B to fire a spike. This illustrates that temporal integration can add a significant delay to the transmission of spikes in a polysynaptic pathway when the latency in transmission is a sum of conduction delay and temporal integration time.

Note that although both neurons B and D are tightly coupled, polysynaptic temporal integration produces less than complete spike-to-spike coupling as revealed by the appearance of points above 15 ms post-CIs during the integration period (i.e., pre-ISI $<$ 10 ms) in Fig. 6 (cf. region *c* of Fig. 3A). Yet, neuron D fires with more regularity than neuron B as revealed by a single primary peak (between 4 and 10 ms) in the ISI histogram (Fig. 4B) and the disappearance of the secondary peak ($>$ 10 ms ISI) when compared

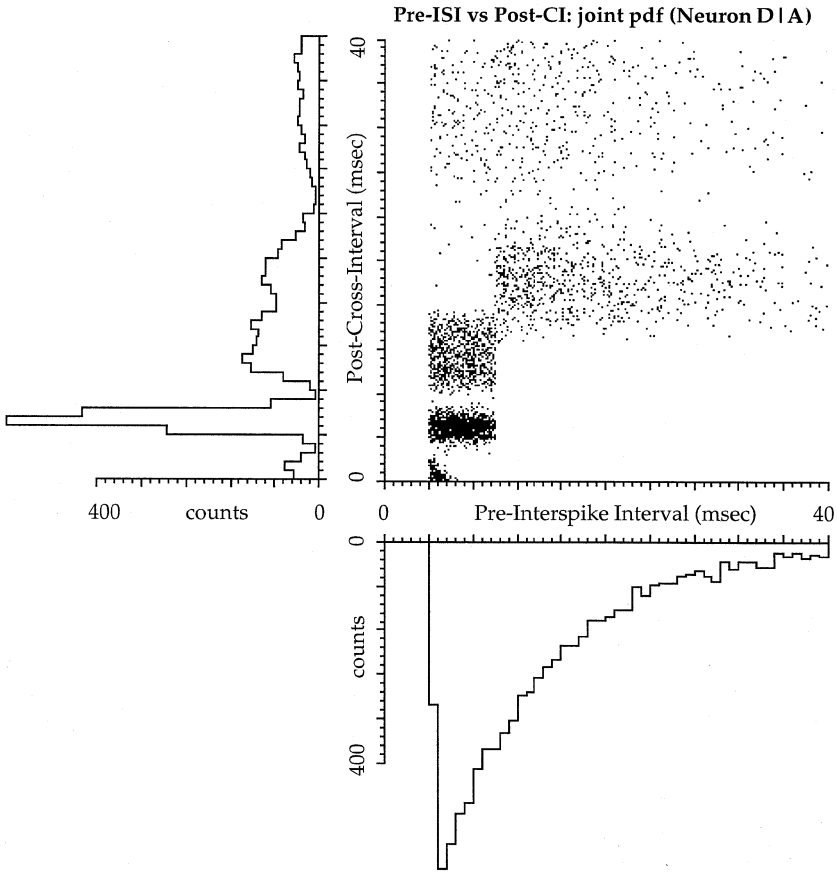

Fig. 6. Pre-ISI vs post-CI scatter plot for neuron A as the reference neuron and the polysynaptically driven neuron D as the compared neuron. Note that the coupling probability is less than 100% during the integration period, as revealed by the points in region *c* (cf. Fig. 3A)

with that of neuron B (see Fig. 4A). This shows that regularity in firing can be enhanced by polysynaptic temporal integration.

3.7 Effects of incomplete coupling during the integration period

The above examples are illustrated with tightly coupled neurons having a finite integration period that ends abruptly. Although nonphysiological, these examples serve the purpose of revealing essential firing features by the pre-ISI/post-CI analyses. We will illustrate the next example with a more physiological integration period. The excitatory coupling probability between the neurons during the integration period of neuron E gradually decreases from 100% at the first 10 ms to 0% at the end of 30 ms. The complete 100% coupling probability at the first 10 ms can be deduced from the fact that no points are found to lie above the horizontal band during the first 10 ms pre-ISI (Fig. 7). Points are found to be gradually scattered above this horizontal band as the pre-ISI increases from 10 ms to 30 ms, reflecting the gradual decrease in coupling strength during the latter phase of the integration period. Thus, this example illustrates the effects of complete and incomplete coupling between neurons during the integration period. The firing pattern of this driven neuron (revealed by the ISI histogram of Fig. 4C) resulting from temporal integration is not as regular in this example as in the previous one (see Fig. 4A) due to the gradual decrease of coupling probability within the integration period.

3.8 Effects of inhibitory temporal integration

To show the effects of temporal integration of inhibition on the firing of a driven neuron, neuron F's firing is simulated with a Poisson process, while inhibited by neuron A (with a suppression period that lasts for 4 ms, and a conduction delay of 1 ms). The pre-ISI/post-CI plot of Fig. 8 reveals this 4 ms inhibition as lack of points in the horizontal band between 1 and 5 ms post-CIs. The integration period of neuron F is similar to that of neuron E with a gradual decrease in coupling probability. This integration period is reflected in the horizontal band where no points are found in the first 10 ms pre-ISI, and points are found to be gradually increasing to its background level at 30 ms. The post-CI histogram (left histogram of Fig. 8) also shows the suppression of firing by neuron A (between 1 and 5 ms), but again, it does not reveal any information about whether this inhibition is correlated with the integration period or not. In contrast, the pre-ISI/post-CI analysis clearly reveals the temporal integration that is associated with the suppression of the firing in a neuron. Not only does this analysis extract the *suppression period* (= 4 ms) from the post-CI axis (i.e., between 1 and 5 ms post-CI), but also the inhibitory temporal *integration period* (= 30 ms) from the pre-ISI axis (i.e., the complete lacking of points in the horizontal band between 4 and 10 ms, and the gradual appearance of points between 10 and 30 ms pre-ISIs).

In contrast to the regularity of spike firing as a result of excitatory temporal integration, inhibitory temporal integration does not produce regularity or periodicity in spike firing.

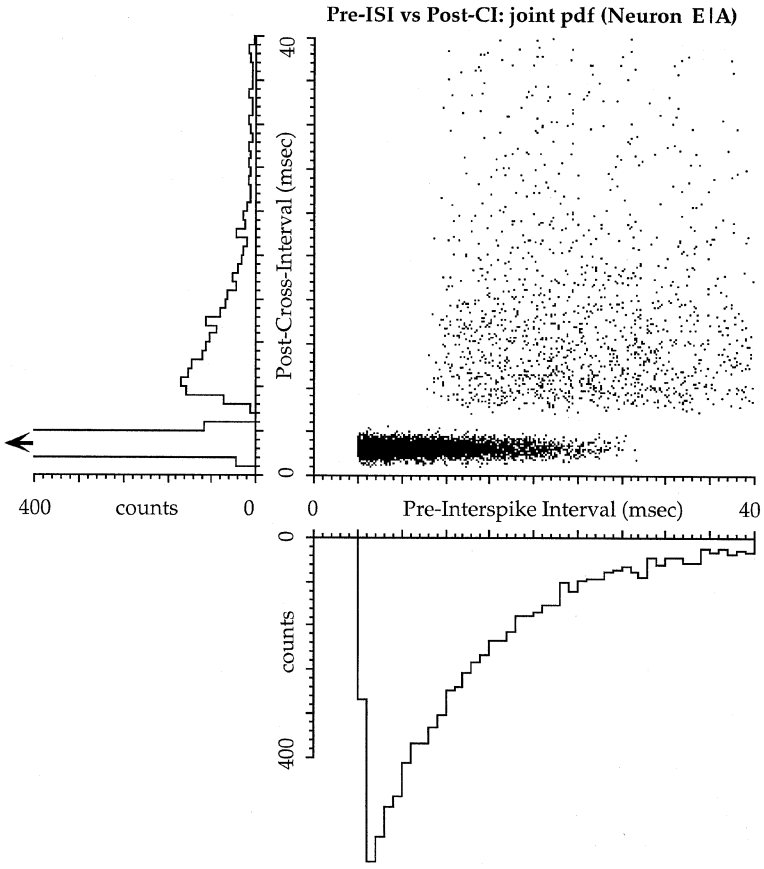

Fig. 7. Pre-ISI vs post-CI scatter plot for neuron A as the reference neuron and neuron E as the compared neuron with gradually decreasing coupling probability strength. The gradual integration period of doublet firing is revealed by the tapering horizontal band of points at 2.5 ms post-CI and the appearance of points above the horizontal band between 10 and 30 ms pre-ISI

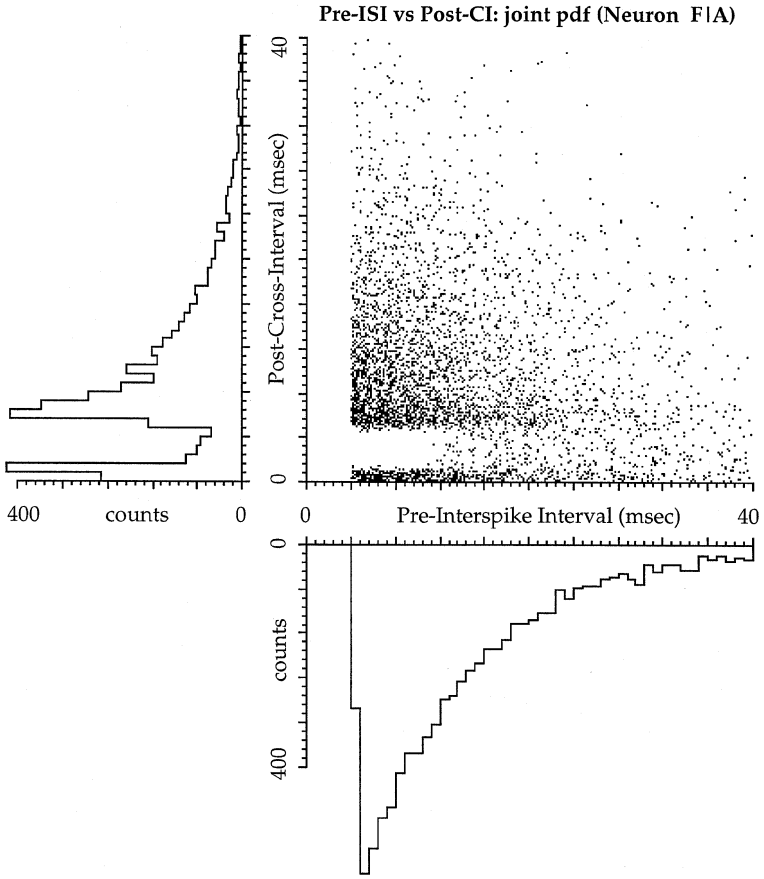

Fig. 8. Pre-ISI vs post-CI scatter plot for neuron A as the reference neuron and neuron F as the compared neuron with inhibitory connection with neuron A. Note the tapering reduction of points along the horizontal band of points at 2.5 ms post-CI reveals the gradual integration period of inhibition due to doublet firing in the presynaptic neuron A

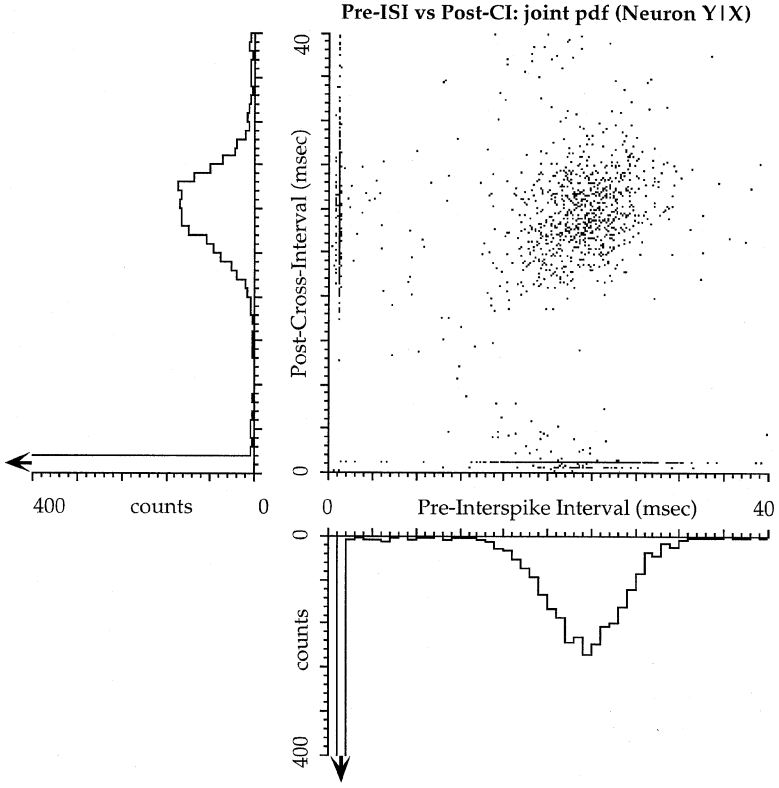

Fig. 9. Pre-ISI vs post-CI scatter plot for biological neuron X as the reference neuron and neuron Y as the compared neuron showing the temporal integration of a doublet firing in neuron X that is coupled with the suppression of firing in neuron Y

This can be deduced from the ISI histogram of Fig. 4D that shows a Poisson-like distribution.

3.9 Effects of temporal integration in biological neurons

Finally, let us apply the analysis to the spike trains recorded from cultured spinal cord neurons. Networks of neurons were cultured on plates with an array of 64-channel photoetched microelectrodes according to the methodology of Gross et al. (1977), similar to that of previous analyses (Gross and Tam 1994; Tam and Gross 1994b). The pre-ISI/post-CI plot for a neuron pair shows two bands of points parallel to the x and y axes as well as a central cluster of points. The ISI histogram (bottom histogram of Fig. 9) reveals that neuron X fired with a doublet ($\sim$ 1 ms ISI) alternating with a longer ISI (peaking at $\sim$ 25 ms). The firing of neuron Y is found to be coupled with neuron X only when X did not fire a doublet. That is, points are found along the horizontal band at 1 ms post-CI only when neuron X fired at longer ISIs (15 $\sim$ 35 ms); but when neuron X fired a doublet (1 ms ISI), just a few points are found at coordinate (1, 1). Alternatively, when neuron X fired a doublet, neuron Y rarely fired at 1 ms latency [as indicated by just a few points at coordinate (1, 1)], but most often fired at longer lag times (i.e., post-CI $>$ 10 ms). This shows that inhibitory temporal integration of the doublet in biological neurons is revealed by this analysis.

4 Discussion

A temporal integration analysis technique is introduced to reveal the likelihood of a spike being generated from the temporal summation of two consecutive spikes by estimating the conditional probability of firing a spike relative to this consecutive firing period needed for temporal integration. This pre-ISI/post-CI analysis provides a statistical measure for estimating the conditional probability of spike firing in a compared neuron in relation to the period of doublet firing in a reference neuron. Alternatively, information theoretics can be used to describe the statistics of neuronal interactions, such as the establishment of the statistical significance of a cross-correlation (Palm 1981), the detection of the synaptic connectivity between neurons (Yamada et al. 1993), and the estimation of the order of a Markov process of neurons (Tsukada et al. 1975; Nakahama et al. 1983). This paper adopts a traditional statistical approach in the analysis rather than the information theoretic approach so that the conditional probability of firing can be obtained to reveal the integration period based on the derived statistics.

Using this analysis, the temporal integration period can be extracted statistically. Simulation examples of different integration periods and latencies are used to illustrate the different effects of temporal integration on the firing characteristics of neurons. The existence and the duration of temporal integration can be deduced from the pre-ISI/post-CI plot as demonstrated in the simulations.

The results clearly show that the pre-ISI/post-CI plot can reveal the duration of temporal integration that is associated with spike generation. Excitatory temporal summation of two spikes is revealed by a horizontal band of points in the pre-ISI/post-CI scatter plot that is limited in duration. In contrast, for inhibitory coupled neurons, the integration period is revealed by the absence of points in a horizontal band with a limited duration.

The analyses show that the effect of temporal integration on the driven neuron for excitatory coupled neurons is very different than the effect for inhibitory neurons. If the neurons are excitatorily coupled, the finite duration of integration periods can produce regularity in spike firing in the driven neuron. In contrast, for inhibitory coupled neurons, the regularity of spike firing is not evident as a result of being suppressed by a randomly incoming firing rate. Thus, the present technique provides an analytical tool to study the effects of temporal integration in a network of neurons since it can detect whether the coupled firing in one neuron is correlated with the *first* preceding spike or the *second-to-last* preceding spike in another neuron.

One of the seemingly unexpected results of temporal integration is that the firing pattern of a driven neuron can be significantly different from that of the driver neuron. This is due to the fact that more than one spike is required for temporal summation. Without temporal summation, the driven neuron can follow the spike firing pattern of the driver neuron with a single-spike to single-spike following rate if the neurons are tightly coupled. With temporal summation, two or more spikes are required to arrive at the synapse successively within a short duration before the next spike will be generated. Thus, the onset of the next spike generation is delayed by the 'waiting-time' (Knox 1974, 1981). Therefore, the firing of the driven neuron will depend on the arrival time of the second or third spike rather than the arrival time of the first spike, i.e., the firing time of the driven neuron will be correlated with the second- or higher-order ISIs of the driver neuron (if these ISIs fall within the integration period) instead of the first-order ISI.

The key factor contributing to the regularity of firing intervals as a result of temporal integration is the *finite* temporal integration period. When the integration period is limited to a finite duration, the longer higher-order ISIs of the incoming spikes will be excluded from the generation of the next spike. In other words, only incoming spikes arriving at intervals within the integration period will be eligible for triggering the generation of the next spike, which is revealed by the present spike-train analysis technique. Thus, temporal integration may act as a bandpass filter in spike signal processing.

Also unexpected is that the regularity of firing can be enhanced by temporal integration in a chain of polysynaptically connected neurons. This polysynaptic enhancement in regularity of firing can be considered as multistage bandpass filtering in neural signal processing.

In conclusion, this paper introduced a new spike-train analysis method for detecting temporal integration of a doublet spike firing in relation to the spike generation of a driven neuron. Also revealed is the difference between the effects of temporal integration on the excitatory neuron and the inhibitory neuron. By using the method introduced in this paper, we have discovered that the regularity of spike firing can be produced as a result of being driven by a randomly firing neuron provided that the integration period is finite in duration. This regularity can further be enhanced by polysynaptic coupling. Also, it is shown that a specific property of a neuron (integration period in this case) can be used to regulate the firing pattern of another neuron, relatively different from the firing pattern of the driver neuron. The bandpass filtering property created by temporally integrating spikes in a chain of neurons is revealed by this analysis. Although this analysis is limited to reveal temporal summation only of a doublet, this is one of the first correlation methods to reveal temporal integration based on spike trains only, without intracellularly recording subthreshold potentials.

Acknowledgements. This research was supported by the Office of Naval Research (ONR grant numbers N00014-93-1-0135 and N00014-94-1-0686) and a Faculty Research Grant from the University of North Texas. I thank Dr. Michelle Fitzurka for her critical review of the manuscript and the use of experimental data, Dr. Gross for the cell culture, and Ms. S. Leanne Betts for editorial assistance.

References

1. Aertsen AMHJ, Gerstein GL, Habib MK, Palm G (1989) Dynamics of neuronal firing correlation: modulation of 'effective connectivity.' J Neurophysiol 61: 900–917
2. Cohen LB, Lesher S (1986) Optical monitoring of membrane potential: methods of multisite optical measurements. Soc Gen Physiol Ser 40: 71–99
3. Droge DH, Gross GW, Hightower MH, Czisny LE (1986) Multielectrode analysis of coordinated, multisite, rhythmic bursting in cultured CNS monolayer networks. J Neurosci 6: 1583–1592
4. Gerstein GL, Bloom MJ, Espinosa IE, Evanczuk S, Turner MR (1982) Design of a laboratory for multineuron studies. IEEE Syst Man Cybern 13: 668–676
5. Gross GW (1994) Internal dynamics of randomized mammalian neuronal networks in culture. In: McKenna T, Stenger DA (eds) Enabling technologies for cultured neural networks. Academic Press, San Diego, pp 277–317
6. Gross GW, Rieske E, Kreutzberg GW, Meyer A (1977) A new fixed-array multimicroelectrode system designed for long-term monitoring of extracellular single unit neuronal activity in vitro. Neurosci Lett 6: 101–105
7. Gross GW, Tam DC (1994) Pre-conditional correlation between neurons in cultured networks. Proc World Congress on Neural Networks, San Diego, 2: 786–791
8. Knox CK (1974) Cross-correlation functions for a neuronal model. Biophys J 14: 567–582
9. Knox CK (1981) Detection of neuronal interactions using correlation analysis. Trends Neurosci 4: 222–224
10. Kudela P, Franaszczuk PJ, Bergey GK (1997) A simple computer model of excitable synaptically connected neurons. Biol Cybern 77: 71–77
11. Melssen WJ, Epping WJM (1987) Detection and estimation of neural connectivity based on crosscorrelation analysis. Biol Cybern 57: 403–414
12. Nakahama H, Yamamoto M, Aya K, Shima K, Fujii H (1983) Markov dependency based on Shannon's entropy and its application to neural spike trains. IEEE Trans Syst Man Cybern 13: 692–701
13. Nakahama H, Yamada S, Shiono S, Maeda M, Satoh F (1992) 448-detector optical recording system: development and application to *Aplysia* gill-withdrawal reflex. IEEE Trans Biomed Eng 39: 26–36
14. Nicolelis MA, Baccala LA, Chapin JK (1995) Sensorimotor encoding by synchronous neural ensemble activity at multiple levels of the somatosensory system. Science 268: 1353–1358
15. Nicolelis MA, Chapin JK (1994) Spatiotemporal structure of somatosensory responses of many-neuron ensembles in the rat ventral posterior medial nucleus of the thalamus. J Neurosci 14: 3511–3532
16. Nicolelis MA, Ghazanfar AA, Faggin BM, Votaw S, Oliveira LM (1997) Reconstructing the engram: simultaneous, multisite, many single neuron recordings. Neuron 18: 529–537
17. Nicolelis MA, Lin RC, Woodward DJ, Chapin JK (1993) Dynamic and distributed properties of many-neuron ensembles in the ventral posterior medial thalamus of awake rats. Proc Natl Acad Sci USA 90: 2212–2216

18. Novak JL, Wheeler BC (1986) Recording from the *Aplysia* abdominal ganglion with a planar microelectrode array. IEEE Trans Biomed Eng 33: 196–202
19. Palm G (1981) Evidence, information, and surprise. Biol Cybern 42: 57–68
20. Palm G, Aertsen AMHJ, Gerstein GL (1988) On the significance of correlations among neuronal spike trains. Biol Cybern 59: 1–11
21. Perkel DH, Gerstein GL, Moore GP (1967a) Neuronal spike trains and stochastic point process. I. The single spike train. Biophys J 7: 391–418
22. Perkel DH, Gerstein GL, Moore GP (1967b) Neuronal spike trains and stochastic point process. II. Simultaneous spike trains. Biophys J 7: 419–440
23. Rodieck RW, Kiang NY-S, Gerstein GL (1962) Some quantitative methods for the study of spontaneous activity of single neurons. Biophys J 2: 351–368
24. Selz KA, Mandell AJ (1992) Critical coherence and characteristic times in brain stem neuronal discharge patterns. In: McKenna T, Davis J, Zornetzer S (eds) Single neuron computation. Academic Press, San Diego, pp 525–560
25. Smith (1992) A heuristic approach to stochastic models of single neurons. In: McKenna T, Davis J, Zornetzer S (eds) Single neuron computation. Academic Press, San Diego, pp 561–588
26. Softky WR, Koch C (1993) The highly irregular firing of cortical cells is inconsistent with temporal integration of random EPSPs. J Neurosci 13: 334–350
27. Tam DC, Ebner TJ, Knox CK (1988) Cross-interval histogram and cross-interspike interval histogram correlation analysis of simultaneously recorded multiple spike train data. J Neurosci Methods 23: 23–33
28. Tam DC, Gross GW (1994a) Dynamical changes in neuronal network circuitries using multi-unit spike train analysis. In: McKenna T, Stenger DA (eds) Enabling technologies for cultured neural networks. Academic Press, San Diego, pp 319–345
29. Tam DC, Gross GW (1994b) Post-conditional correlation between neurons in cultured neuronal networks. Proc World Congress on Neural Networks, San Diego, 2: 792–797
30. Tsukada M, Ishii H, Sato R (1975) Temporal pattern discrimination of impulse sequences in the computer-simulated nerve cells. Biol Cybern 17: 19–28
31. Yamada S, Nakashima M, Matsumoto K, Shiono S (1993) Information theoretic analysis of action potential trains. Biol Cybern 68: 215–220
32. Yang X, Shamma SA (1990) Identification of connectivity in neural networks. Biophys J 57: 987–999